Compact UWB MIMO Filtennas with Dual Bandnotch, High Isolation and High Diversity

Ahmad, W., Tasic, M. and Budimir, D.

Compact UWB MIMO Filtennas with Dual Bandnotch, High Isolation and High Diversity

Waqas Ahmad [#1], Miodrag Tasic [*2], and Djuradj Budimir [#3]

[#] *Wireless Communications Research Group, University of Westminster*
115 New Cavendish Street, London, W1W 6UW, United Kingdom
[3] d.budimir@westminster.ac.uk
[*] *School of Electrical Engineering, University of Belgrade*
Belgrade, Serbia

Abstract- **This paper presents a 4x4 MIMO filtenna aimed for use with UWB applications. The MIMO filtenna is simulated, fabricated and measured. Obtained simulation and measurement results agree well with each other and have been presented to validate the accuracy of the proposed structure. Measured passband is 2.96–11.56 GHz, with dual bandnotch at 3.5 GHz (S_{11} = -1.25 dB) and 6.05 GHz (S_{11} = -2.4 dB). Measured isolation is more than 20 dB between all individual elements of the MIMO filtenna. The behaviour of current within the filtenna at the bandnotch frequencies has been shown. Elements of the filtenna exhibit bi-directional radiation patterns in the E-plane and omnidirectional patterns in the H-plane. The gain and efficiency have also been presented; with the average values being 5.3 dBi and 90% respectively. The Envelope Correlation Coefficient has been calculated from both simulations and measurements; with the measured values being below 0.001 for the passband.**

I. INTRODUCTION

UWB technology has constantly been a hot research area in recent times due to its inherent advantages, such as low-power and high data transfer rate within a limited range. However, the 3.1–10.6 GHz UWB overlaps various interfering services which have to be rejected [1]. The combination of UWB technology and MIMO technology is an interesting research orientation [2]. Various MIMO filtennas for UWB systems have been proposed [3]–[7]. But these do not satisfy the main challenges in MIMO filtenna design, such as placing multiple elements closely while maintaining a high isolation, wide operation band and rejection of interfering bands. In this paper, a four element MIMO filtenna is proposed. The filtenna satisfies all challenges. It is able to reject the unwanted WiMAX and WLAN bands. It is more compact than [3] by 11.8%, [4] by 31.6%, [5] by 38.4%, and [6] by 67.3%. A high isolation has been achieved; better than [4]–[6] by 5 dB and [7] by 12 dB. The diversity performance is better than [4] and [5].

II. DESIGN OF PROPOSED MIMO FILTENNAS

The MIMO filtenna is formed by laying four individuals filtenna elements adjacent to each other, with each consecutive element rotated 90° clockwise to the left of the adjacent one. Such a layout results in a square 4x4 configuration as illustrated in Fig. 1. Each element is symmetrical with respect to its longitudinal direction. The filtenna is designed with a mid-band frequency of 6.85 GHz. All elements are inductively

coupled to the source and are excited via ports 1, 2, 3, and 4; with all 50 Ω feedlines. The structure utilises a defected ground structure with a partial ground plane of length 13.1 mm for each element. For each element's top radiating patch, a spade shape is chosen. Between every element's spade patch and the feedline, lie two rectangular patches of different sizes. These improve impedance matching and also provide good characteristic matching at the higher frequencies. Due to the steady change in structure of the radiating patches of this shape, a broadband impedance bandwidth is easily achieved. These also provide a smooth shift from one resonant mode to another. The 3.5 GHz bandnotch is formed by a circular resonator laid within the top patch. The 5.8 GHz bandnotch is produced by two rectangular resonators; each laid on either side of the feedlines. A splitting gap is present in the resonators from where current is able to flow in the inner side of the resonators. All resonators are $0.5\lambda_g$ long; where λ_g is the guided wavelength at their respective bandnotch frequency. The filtenna has a total compact size of 78 mm x 78 mm; equivalent to $1.02\lambda_g$ x $1.02\lambda_g$, where λ_g is the guided wavelength at the lower frequency of 3.1 GHz. The gap between each adjacent element is G1 i.e. 3.1 mm ($0.04\lambda_g$).
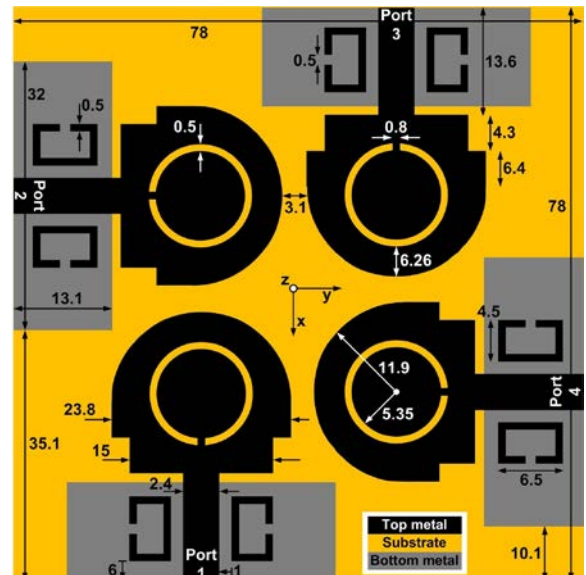

Figure 1. Geometry of the MIMO filtenna.

The structure is designed on a 0.795 mm thick Rogers RT5880 substrate of a dielectric permittivity 2.2 and a loss factor 0.0009. The designed filtenna was simulated using the commercial software CST Microwave Studio, fabricated and measured using an Agilent E8361A PNA Network Analyser.
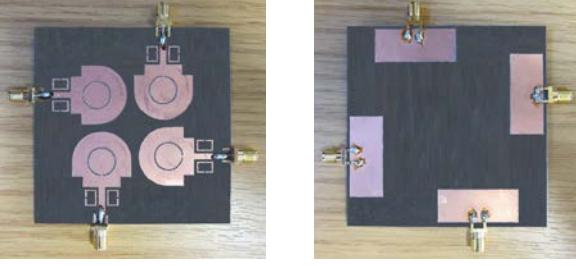

Figure 2. Photographs of top and bottom side of the fabricated MIMO filtenna.

A. Return Loss

The return loss of the MIMO filtenna is shown in Fig. 3. Simulation shows that a full bandpass response at a return loss of more than 10 dB is obtained in the 2.69–12.29 GHz range. Measurements were acquired by stimulating each port one by one while, at the same time, the other three ports were terminated using 50 Ω loads. Measurements show the average passband of all four elements to be from 2.96–11.56 GHz. Within this measured range, there is negligible difference amongst the individual elements' lower passband frequency and an average difference of ±0.98 % amongst each element's upper passband frequency. The simulated dual bandnotch have been attained at 3.45 GHz (S_{11} = -0.5 dB) and 6.04 GHz (S_{11} = -1.4 dB). Measurements show the dual bandnotch at the slightly shifted frequencies of 3.52 GHz (S_{11} = -1.25 dB) 6.05 GHz (S_{11} = -2.4 dB). There is negligible difference amongst the bandnotch frequencies of each element. The difference in the simulated and measured results is due to the fabrication tolerances and tolerances of the materials used. Another valid reason is the untreated currents on the SMA connectors.
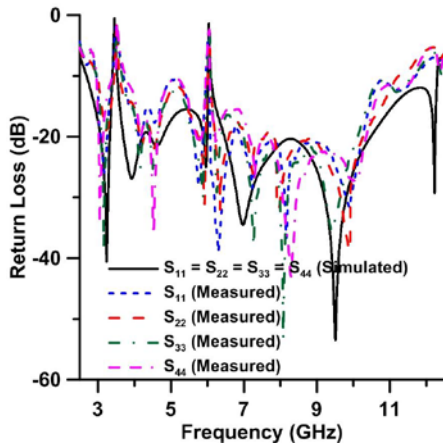

Figure 3. Return loss of the MIMO filtenna.

B. Isolation

The simulated and measured results of isolation between adjacent elements of the MIMO filtenna are given in Fig. 4, while those of opposite elements are given in Fig. 5. Measurements were obtained by exciting each port while, at the same time, the other three ports were terminated using 50 Ω loads. Measurements show the isolation to be more than 20 dB in all of the passband in both cases. At 4.25–4.4 GHz, as seen from both figures, the isolation comes to being very close to less than 20 dB. This could be easily increased by placing a stub or a multi-mode resonator in the middle of the filtenna, of a quarter wavelength size at 4.33 GHz and connecting the four radiating elements or the ground planes to it [6]. This would result in the current at 4.33 GHz being focused only on the stub/resonator. It is also possible to further improve the overall isolation of the MIMO filtenna, but this would be at the cost of deterioration in the overall return loss of the filtenna [3].
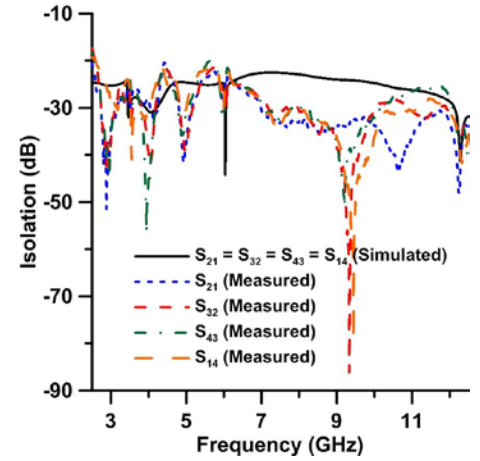

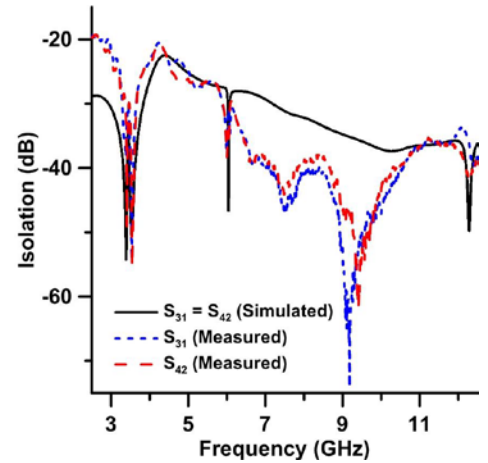Figure 4. Isolation between adjacent elements of the MIMO filtenna.

Figure 5. Isolation between opposite elements of the MIMO filtenna.

C. Distribution of Surface Currents

In order to further explain the effects of the three resonators on the passband and how each of the bandnotch is achieved, the simulated distribution of surface currents at the two bandnotch frequencies of 3.5 GHz and 5.8 GHz is given in Fig. 6 and Fig. 7 respectively. At 3.5 GHz, most of the current is concentrated around the circular resonators. While at 5.8 GHz, majority of the current is focused around the rectangular resonators. At these two frequencies, the direction of the flow of the current along the inner and outer edges of the resonators is opposite to one another. Thus, the currents are cancelled by each other and the filtenna does not radiate and stopband characteristics, i.e. bandnotch, are achieved.
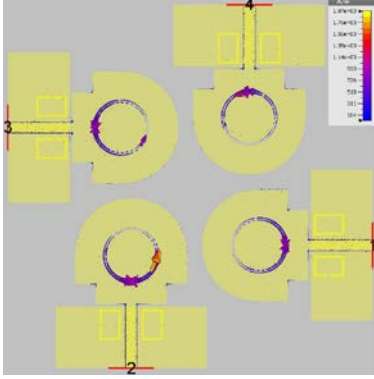

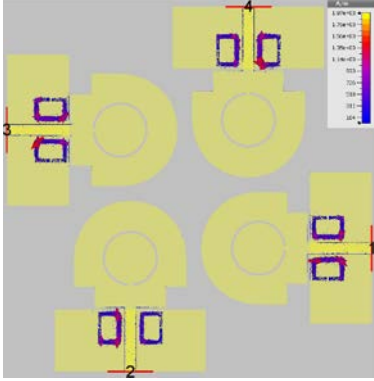Figure 6. Distribution of surface currents at 3.5 GHz.

Figure 7. Distribution of surface currents at 5.8 GHz.

D. Pattern Diversity, Radiation Patterns, Gain, and Efficiency

Because of the orthogonal shape of the structure, the MIMO filtenna is able to achieve radiation patterns diversity. In all three planes, i.e. xz, yz and xy-planes, the patterns of elements 1 and 2 are the mirror transforms of the patterns exhibited by elements 3 and 4 respectively. This also means that element 1's patterns in xz-plane and yz-plane are the same as those of element 2's patterns in the yz-plane and xz-plane respectively. Same relationship is between elements 2 and 3, elements 3 and 4, and elements 4 and 1. Similarly in the xy-plane, all patterns are same in magnitude, but rotated +90° clockwise of the

previous element's xy-plane. Because of these relationships, it is sufficient to check the patterns with just one port excited.

The radiation patterns, with port 1 excited and the other three ports terminated with 50 Ω loads, at various frequencies in the E-plane and the H-plane were simulated and measured. The results in Fig. 8 show bidirectional patterns in the E-plane and omnidirectional patterns in the H-plane. A reasonable agreement between the simulation and measurement is seen.
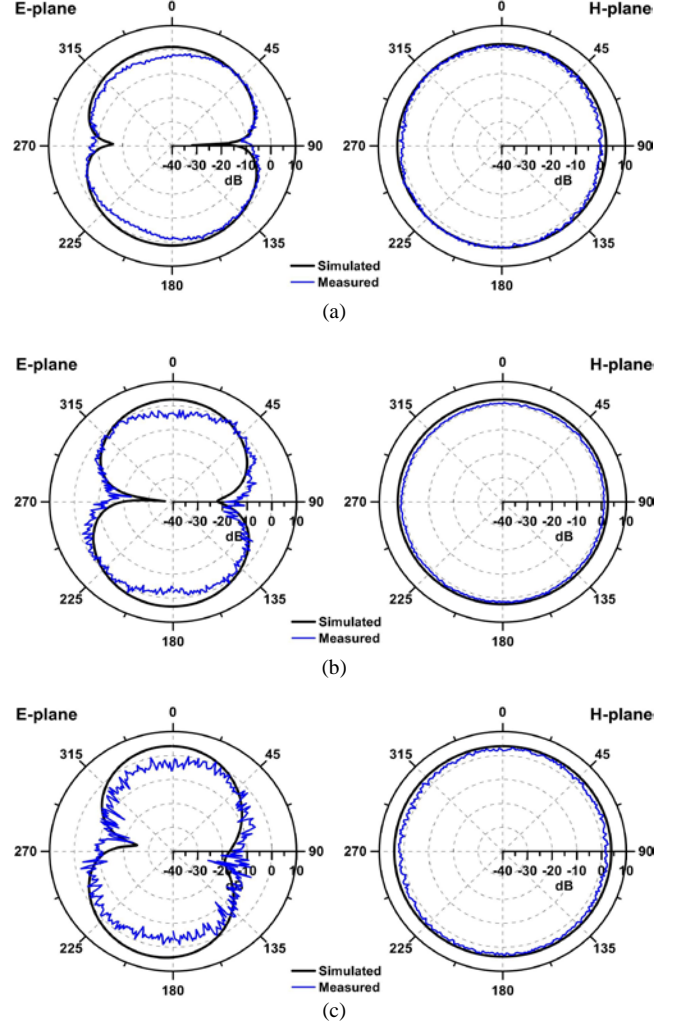

Figure 8. Radiation patterns at (a) 3.1 GHz, (b) 4 GHz and (c) 5.75 GHz.

The simulated gain and efficiency of the structure, both with only port 1 excited and, as well as, all ports excited, is presented in Fig. 9. Results show that the variance of the filtenna gain across the passband is within 3 dBi. The average gain and average efficiency is 5.28 dBi and 90.2 % respectively. Since the filtenna does not radiate at the dual bandnotch frequencies, the gain and efficiency at these drop.

E. Diversity Performance

The Envelope Correlation Coefficient (ECC) is an important parameter for evaluating the diversity performance for filtennas intended for MIMO applications. According to the

method proposed in [8], for four-port lossless MIMO filtennas in uniform propagation environment, the ECC can be calculated by the formula given in (1); where i and j denote the port numbers 1, 2, 3, or 4 and $i \neq j$.

$$\rho_e = \frac{\left|S_{ii}^* S_{ij} + S_{ji}^* S_{jj}\right|^2}{(1 - \left|S_{ii}\right|^2 - \left|S_{ji}\right|^2)(1 - \left|S_{jj}\right|^2 - \left|S_{ij}\right|^2)} \qquad (1)$$

The simulated and measured ECC of adjacent elements are plotted in Fig. 10 and those of opposite elements are plotted in Fig. 11. In the two figures, when a curve exceeds the y-axis limit, the maximum value is indicated by an arrow for clarity purposes. For the obtained passband range of 2.96–11.56 GHz, measured ECC for both the adjacent and opposite elements is below 0.001; while at the bandnotch frequencies, measured ECC is up to a maximum of 0.024 for the adjacent elements and 0.0045 for the opposite elements. Since $\rho_e < 0.25$ for a good diversity performance [2], the obtained values are low enough to ensure a good diversity performance. Moreover, the obtained ECC is lower than those presented in [4] and [5], where the maximum values are 0.025 and 0.04 respectively.
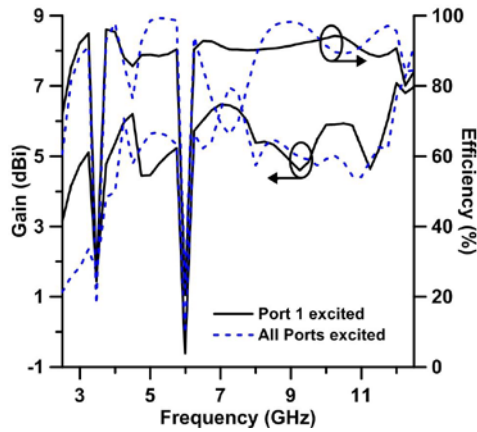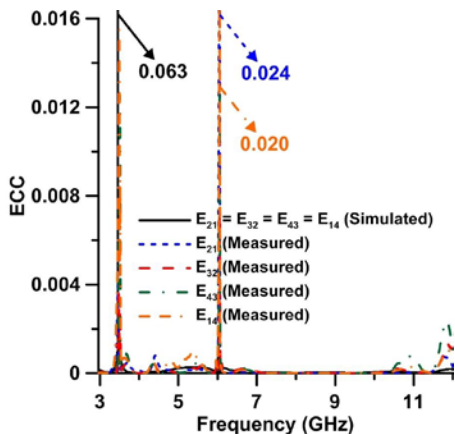

Figure 9. Gain and efficiency of the MIMO filtenna.

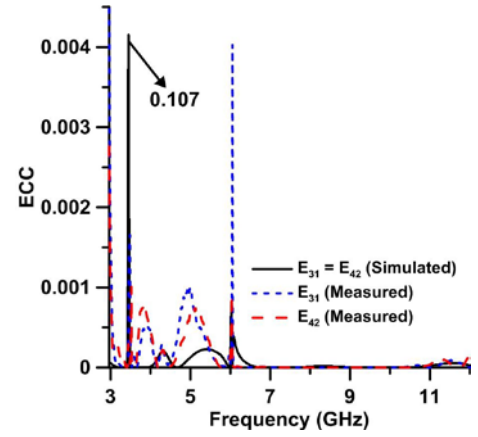Figure 10. ECC between adjacent elements of the MIMO filtenna.

Figure 11. ECC between opposite elements of the MIMO filtenna.

IV. CONCLUSION

A four-port MIMO filtenna for UWB systems has been designed and presented. Simulation and measurement results of the filtenna have been provided. A full UWB passband measuring 2.96–11.56 GHz has been obtained. Within this passband, a high rejection measuring 1.25 dB and 2.4 dB at the WiMAX band and WLAN band respectively has been attained for all individual elements of the MIMO filtenna. A high isolation, measuring more than 20 dB, has been achieved between each element. Additionally, the filtenna has been shown to meet the minimum criteria for MIMO diversity; since it is able to achieve a high diversity performance. Even though some differences between the simulated and measured results are present, these can be optimised. Future work on this MIMO filtenna could include integrating reconfigurability, thereby controlling the behaviour of the undesired bands.

REFERENCES

[1] FCC, "Revision of part 15 of the commission's rules regarding ultra-wideband transmission systems," *First Note and Order Federal Communications Commission*, pp. 98–153, February 2002.
[2] T. Kaiser, F. Zheng, and E. Dimitrov, "An overview of UWB systems with MIMO," *IEEE Proceedings*, vol. 97, no. 2, pp. 285–312, Feb. 2009.
[3] J-F. Li, Q-X. Chu, Z-H. Li, and X-X. Xia, "Compact dual band-notched UWB MIMO antenna with high isolation," *IEEE Transactions on Antennas and Propagation*, vol. 61, no. 9, pp. 4759–4766, Sep. 2013.
[4] X-L. Liu, Z-D. Wang, Y-Z. Yin, J. Ren, and J-J. Wu, "A Compact UWB MIMO antenna using QSCA for high isolation," *IEEE Antennas and Wireless Propagation Letters*, vol. 13, pp. 1497–1500, 2014.
[5] J. Ren, W. Hu, Y. Yin, and R. Fan, "Compact printed MIMO antenna for UWB applications," *IEEE Antennas and Wireless Propagation Letters*, vol. 13, pp. 1517–1520, 2014.
[6] N. K. Kiem, H.N. B. Phuong, Q. N. Hieu, and D. N. Chien, "A compact printed 4×4 MIMO-UWB antenna with WLAN band rejection," *IEEE International Symposium on Antennas and Propagation (APS-URSI 2013)*, pp. 2245–2246, July 2013.
[7] Y. Li, W. Li, C. Liu, and T. Jiang, "Two UWB-MIMO antennas with high isolation using sleeve coupled stepped impedance resonators," *Asia-Pacific Conference on Antennas and Propagation*, August 2012.
[8] S. Blanch, J. Romeu, and I. Corbella, "Exact representation of antenna system diversity performance from input parameter description," *IET Electronics Letters*, vol. 39, no. 9, pp. 705–707, May 2003.